

Dielectric and optical properties close to the percolation threshold. II.

F. Brouers

Institut de Physique, Université de Liège, Sart Tilman 4000 Liège, Belgium

J. P. Clerc, G. Giraud, J. M. Laugier,* and Z. A. Randriamantany†

Département de Physique des Systèmes Désordonnés, Université de Provence, Centre de St. Jérôme, Marseille, France

(Received 2 April 1992)

We present a two-dimensional simulation of the optical properties of granular metal films using the Frank and Lobb algorithm. The results are compared with the effective-medium approximation (EMA). Close to the percolation threshold we obtain excellent agreement between the simulation and the EMA. It is shown that the anomalous absorption in the near ir stems from the broadened spectrum of surface-plasmon (or cluster) modes and the percolation scaling law for a mixture of two conductors. This model is able to account for the absorption, reflection, and transmission of thin semicontinuous gold films and their frequency independence at the optical percolation threshold. The discrepancy between EMA and the simulations and experimental data at the edges of the cluster-mode spectrum and in the Lifshitz tails outside the critical region are due to configuration fluctuations neglected in the EMA.

I. INTRODUCTION

The optical and infrared properties of random metal-insulator composites (thin films or cermets) close to the percolation threshold have been the subject of a number of recent works (for a review see Ref. 1). The optical properties of these materials are characterized by a number of features that do not appear in the pure metal. The main difference for noble and other good conductors based composites is the occurrence of a spectrum of Mie or "surface plasmon" absorption resonances in the visible or near-infrared frequency range, which depends on the morphology of the metallic inclusions in the composite. As the concentration of inclusions increases this spectrum (whose maximum for noble metals lie in the visible range) broadens towards higher wavelengths due to the formation of clusters of various shapes and sizes.² A discussion of the mathematical properties of the spectrum of resonances in resistor-inductor-capacitor (RLC) networks simulating such composite systems is presented in Ref. 3.

In this paper we are dealing with the optical properties of semicontinuous noble-metal films for which well-documented experimental data are available. In these films near the percolation threshold p_c the cluster resonances give rise to an unusual behavior of the film reflectivity and transmittivity. In the near-infrared region ($\sim 2 \mu\text{m}$) one observes three characteristic features:⁴⁻¹⁰ (1) The absorptance, reflectance, and transmittance are almost frequency independent in the vicinity of the percolation threshold. (2) There is no sharp transition of the reflectivity at the metal-insulator transition. The observed reflectance is much lower than that of a continuous metallic film but increases almost linearly with the metal filling factor. (3) The absorption is maximum in the vicinity of the percolation threshold and is much higher than that of a continuous film of the same electronic density.

These nontrivial results have been used to question the validity of mean-field theories to describe the optical

properties of composites in the vicinity of the metal-insulator transition. Recently a few models¹⁰⁻¹³ have been proposed, which make an extensive use of the various scaling laws and ansatz of the percolation theory. Authors of Ref. 11 assume that only clusters larger than the light wavelength λ contribute to the absorption. Authors of Ref. 13 identify the wide region of strong absorption as the region where the anomalous diffusion length (much smaller than λ) on the percolating backbone is smaller than the percolation correlation length. In these works, the quantitative comparison with experiment depends on the ansatz chosen for the cluster distribution or the values of the unknown expansion coefficients of the scaling functions. In both works the contribution of cluster or surface-plasmon modes are neglected.

The models of Refs. 11-13 assume that over a wide range of filling factors around the percolation threshold p_c , the optical properties are dominated by the fluctuations and therefore cannot be described by an effective dielectric function. If this statement would be confirmed this would cause a serious setback to the efforts undertaken to model the dielectric and electrical properties of composites.^{17,26} It would be also a rare example of a phase transition exhibiting a wide critical region on both sides of the critical point very far from the condition ($p = p_c, \omega = 0$) where a sharp phase transition occurs.

By contrast, it has also been shown¹⁴⁻¹⁶ that the effective-medium theory¹⁷ (EMA) is obeying the good-bad conductor scaling law of Efros and Shklovskii¹⁸ and Straley¹⁹ in the case of a two-dimensional (2D) metal-dielectric composite in the frequency range of interest. As a consequence, the near-infrared optical absorption coefficient is maximum and almost exactly frequency independent for a filling factor p^* (the optical threshold) slightly higher than the percolation threshold p_c in the case of noble-metal films.¹⁵ At p_c the optical resonant absorption from the finite-size clusters starts to decrease and the metallic absorption from the percolating cluster starts to increase. At p^* the sum of these two contribu-

tions is maximum and independent of frequency.¹⁶ These results have been confirmed by real RLC circuits simulations of metal-insulator composites as well as by computer simulations using the transfer matrix methods.^{3,14} On a more theoretical ground, Luck²⁰ using a perturbative expansion of the conductivity has provided a quantitative explanation of the currently observed fact that for a large class of conductance distribution, EMA predictions are very accurate.

In order to try to resolve the contradictions between the conclusions of these two series of works and to clarify the importance and the role of fluctuations as well as the importance of size effects and the role of cluster resonant modes, we present here the results of a numerical simulation using the Frank and Lobb algorithm,²¹ which allows us to calculate the optical absorption coefficient and the reflectivity coefficient for a model of gold-insulator discontinuous thin film. The results of the simulation are compared with the corresponding curves obtained in the EMA. This algorithm has been shown to work efficiently not only for problems involving the conductivity but also for calculating the critical current of a normal metal-superconducting composite. The same method has been used successfully to simulate far-infrared absorption in two-dimensional normal metal-superconductor composites. In that case, the analytical EMA is in excellent agreement with all the results of the simulations.²² The present paper finds its inspiration in the work of Stroud and co-workers²³ who have proposed a similar approach for optical absorption but did not apply it to real systems. In the near ir frequency region, the simulations and calculations we present here allow us to understand the variation of the relative contributions of all the finite clusters and the percolating cluster to the total optical absorption. In the near infrared region we do not find any length scale dependence of the absorption but with our simulations we can recover in the dc regime the finite-size percolation critical exponent t/ν . Although we did not choose the model parameters to fit perfectly the experimental results, the absorption coefficient and reflectivity coefficient curves as well as the reflectance, absorptance, and transmittance of a granular thin film calculated using the Abeles²⁴ formula and reported here are good illustrations and of what is observed in noble-metal discontinuous films around p_c .^{7,12,13} The results of this simulation confirm the findings on the optical conductivity close to p_c and reported in a first paper with the same title¹⁶ and referred to as paper I in the following.

As we shall argue, the agreement between the 2D simulations and the 2D EMA is the consequence of the fact that the relevant exponents in the scaling function valid in the near ir frequency range are the same in the percolation theory and in the EMA. This is not the case in 3D systems and therefore discrepancies are expected for 3D composites although the analytical form of the scaling function should be well approximated by the EMA scaling function.

II. THE MODEL

To simulate the absorption and reflectivity properties of a 2D metal-dielectric composite (cf. paper I), we con-

sider a square lattice occupied by bonds of conductance $\sigma_m(\omega)$ with probability p and bonds of conductance $\sigma_d(\omega)$ with probability $1-p$. The metal conductance $\sigma_m(\omega)$ is the Drude conductivity

$$\sigma_m(\omega) = \frac{\sigma_m(0)}{1+i\tau\omega} + i\omega\epsilon_0\epsilon_m(\infty) \quad (1)$$

and the frequency-dependent dielectric conductance $\sigma_d = i\epsilon_0\epsilon_d\omega$.

The Drude dc conductivity $\sigma_m(0) = \epsilon_0\tau\omega_p^2 = \tau ne^2/m$. The constants ϵ_0 , ϵ_d , and ϵ_m are respectively the vacuum, the dielectric, and the metal closed-shell dielectric constants. The quantities τ^{-1} and ω_p are the metal relaxation and plasmon frequencies. The metal and the insulator are represented by local quantities and in this circuit-like model, propagation effects have been neglected.

To find the bulk conductance of such lattice, the Frank and Lobb (FL) algorithm consists in a repeated application of a sequence of series, parallel and star-triangle $Y-\nabla$ transformations to the bonds of the lattice. The final result of this sequence of transformations is to reduce any finite portion of the lattice to a single bond that has the same conductance as the entire lattice. The average of this conductance over a number of random configurations is the quantity Σ_{FL} from which we will calculate the optical absorption. The efficiency of that algorithm has been analyzed in detail in Ref. 25. It appears that the FL method is best behaved for problems where the conductivity must be calculated for the entire range of filling factor p . In this paper we will compare the results of the FL algorithm numerical simulations with the effective-medium approximation¹⁷ (EMA) solution of

$$p \frac{\Sigma(\omega) - \sigma_m(\omega)}{\sigma_m(\omega) + (d-1)\Sigma(\omega)} + (1-p) \frac{\Sigma(\omega) - \sigma_d(\omega)}{\sigma_d(\omega) + (d-1)\Sigma(\omega)} = 0, \quad (2)$$

where the lattice dimensionality is $d=2$. This self-consistent equation is identical to the Bruggeman approximation for a 2D composite when the depolarization factor is $g=1/d$ and corresponds to circular inclusions in a 2D medium.

Since we are interested in noble-metal discontinuous films and to make possible comparisons with previous papers, we have used for our simulation calculations the same value as in Refs. 26 and 27 and paper I for a gold-based composite metal and dielectric conductances, i.e., $h\omega_p = 9.2$ eV for the plasmon energy, $h/\tau = 0.06$ eV for the relaxation energy. The dielectric constants are $\epsilon_m(\infty) = 6.5$ and $\epsilon_d = 2.82$.

We have calculated Σ_{FL} for square lattices of linear size $L=10, 15, 20, 25, 30, 35,$ and 50 and averaged over 1000 to 10 000 random lattice configurations for various metallic concentrations p . In that model, the infinite lattice percolation threshold is $p_c = 0.5$. From Σ_{FL} we can calculate the real and imaginary part of the dielectric constant ϵ_1 and ϵ_2 given by $\text{Re}\Sigma = \omega\epsilon_0\epsilon_2$ and $\text{Im}\Sigma = \omega\epsilon_0\epsilon_1$. This allows us to calculate the optical conductivity (or optical absorption coefficient^{5,7}) defined by the opticians

as ε_2/λ and the reflection coefficient (for a semi-infinite medium)

$$r = \frac{(n_1 - 1)^2 + n_2^2}{(n_1 + 1)^2 + n_2^2} \quad \text{with } n = \sqrt{\varepsilon_1 + i\varepsilon_2} = n_1 + in_2. \quad (3)$$

We have computed r in two different ways: (a) For each configuration we have calculated the reflectivity coefficient r and then calculate the average r_a ; (b) alternatively, we can calculate the average r_b from the average conductance Σ_{FL} . The usual absorption coefficient η , i.e., the fraction of energy absorbed in passing through unit thickness of the materials, is given by $\eta = 2n_1 n_2 \omega / c = 2\pi\varepsilon_2/\lambda$.

III. NUMERICAL RESULTS

The results of the simulations are illustrated in Figs. 1–5. Figure 1(a) shows the ir optical absorption ε_2/λ (in μm^{-1}) for three wavelengths $\lambda_1 = 2.2$, $\lambda_2 = 1.7$, and $\lambda_3 = 1.5$ μm calculated with the FL algorithm. The linear size of the circuits is 25. We have averaged over 1000 circuit configurations. For $(p - p_c)/p_c < 0$, the contribution to the optical absorption comes essentially from cluster resonant modes, while for $(p - p_c)/p_c > 0$, the absorption comes from both cluster modes and percolating conducting electrons. The optical absorption is maximum for a concentration p^* slightly higher than p_c . As the wavelength increases, the contribution of conducting electrons increases, while the contribution of cluster modes decreases. This explains the narrowing of the central absorption curve around the origin ($p \sim p_c$) and the increase of the absorption for $(p - p_c)/p_c \rightarrow 1$ as the wavelength increases. It is worth noticing that the ε_2/λ is wavelength independent in the immediate vicinity of p_c .

Figure 1(b) shows the optical absorption coefficient ε_2/λ for $\lambda = 1.7$ μm , one of the cases of Fig. 1(a) compared with the results of the mean-field theory (EMA). The behavior is qualitatively the same. However the maximum is closer to $p = p_c$ and the width of the central peak is narrower in the EMA. The mean-field theory does not account properly for the tails of the cluster resonant modes distribution (Lifshitz modes) because it neglects fluctuations coming from rare cluster configurations.

In Fig. 1(c) we show the variation of the optical absorption coefficient for $\lambda = 1.7$ μm with the lattice linear size L . As L increases, the width of the “anomalous” central region broadens and tends quite rapidly towards a stabilized curve.

Figure 2 reproduces the results of Fig. 1(b). The EMA linear contribution from percolating conducting electrons has been subtracted to emphasize the contributions of resonant cluster modes. Close to p_c the variation of percolating electrons conductivity is no longer linear but $\sim (p - p_c)^{1.3}$ and this explains the fact that the central peak in the FL simulation is slightly asymmetric with respect to the origin ($p = p_c$).

Figure 3(a) gives the variation of the optical absorption coefficient with λ for $p = p_c = 0.5$ and for increasing lat-

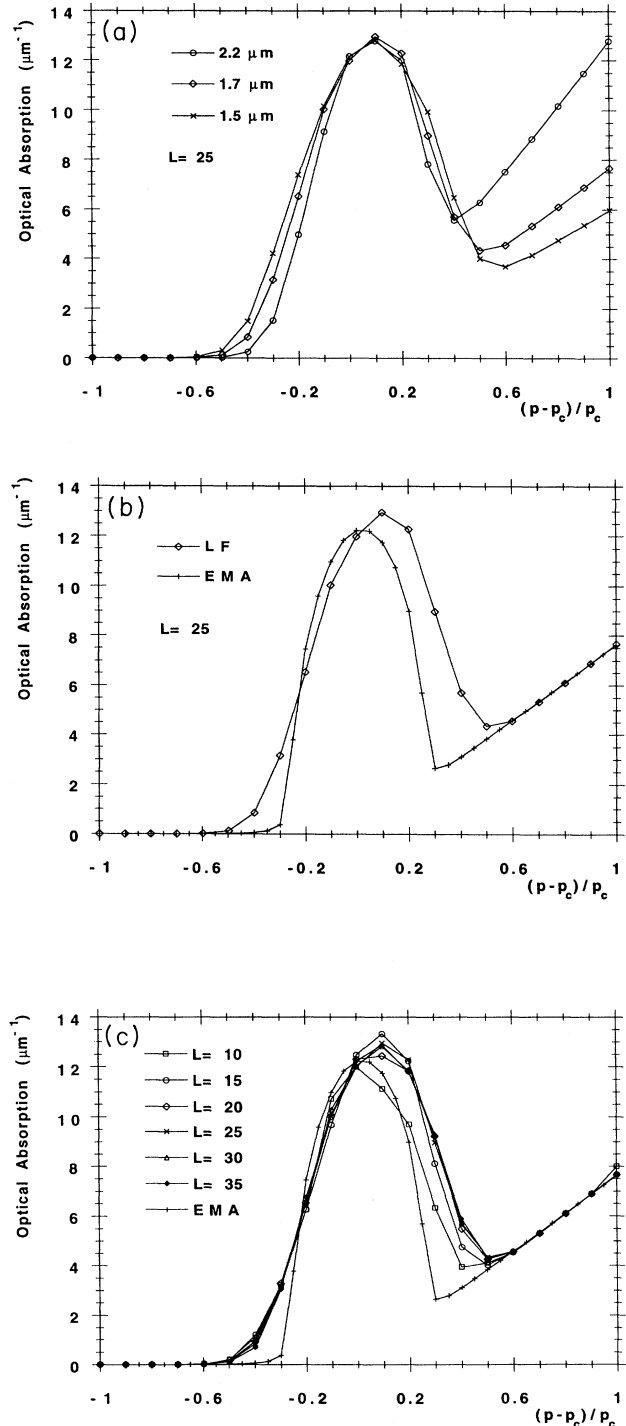


FIG. 1. (a) Near-infrared optical absorption for three wavelengths 2.2, 1.7, 1.5 μm calculated with the FL algorithm for circuits of linear size 25 (averaged over 1000 realizations) as a function of metal coverage. (b) Near-infrared optical absorption for $\lambda = 1.7$ μm , calculated with the FL algorithm for circuits of linear size 25 and compared with the results of the mean-field theory (EMA). (c) Near-infrared optical absorption for $\lambda = 1.7$ μm , calculated with the FL algorithm for circuits of various linear size (from $L = 10$ to 35).

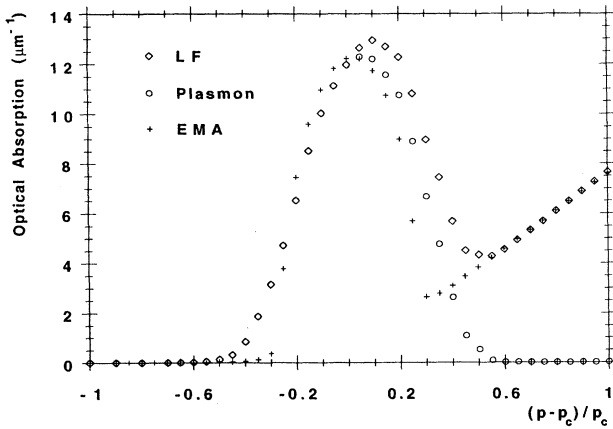


FIG. 2. The same results of Fig. 1(b). The contributions of resonant modes and conducting electrons have been separated.

tice sizes. For very small L , size effects start to appear for large λ outside the anomalous absorption region.

In Fig. 3(b) we show the same curve for $p^* = 0.5057$, the optical threshold in the EMA, calculated with the FL algorithm ($L = 25$) and in the EMA. Figures 3(a) and 3(b) show that near p_c , the optical absorption coefficient is practically wavelength independent. In that region, the EMA is in surprisingly good agreement with the results of the FL simulations.

Figure 4(a) illustrates the variation with $(p - p_c) / p_c$ of the calculated reflection coefficients r_a and r_b and r_{EMA} for $\lambda = 1.7 \mu\text{m}$. As for the case of the optical absorption, the agreement between the EMA and FL simulation is quite remarkable between -0.2 and 0.2 . The discrepancy in the region $\pm(0.25-0.50)$ is due to the fact that the EMA is not appropriate to deal with the tails of the cluster resonant modes distribution. In Fig. 4(b), we show the variation of the reflection coefficients at $p = p_c$ for a range of ir wavelengths.

The results presented so far are only meaningful if the

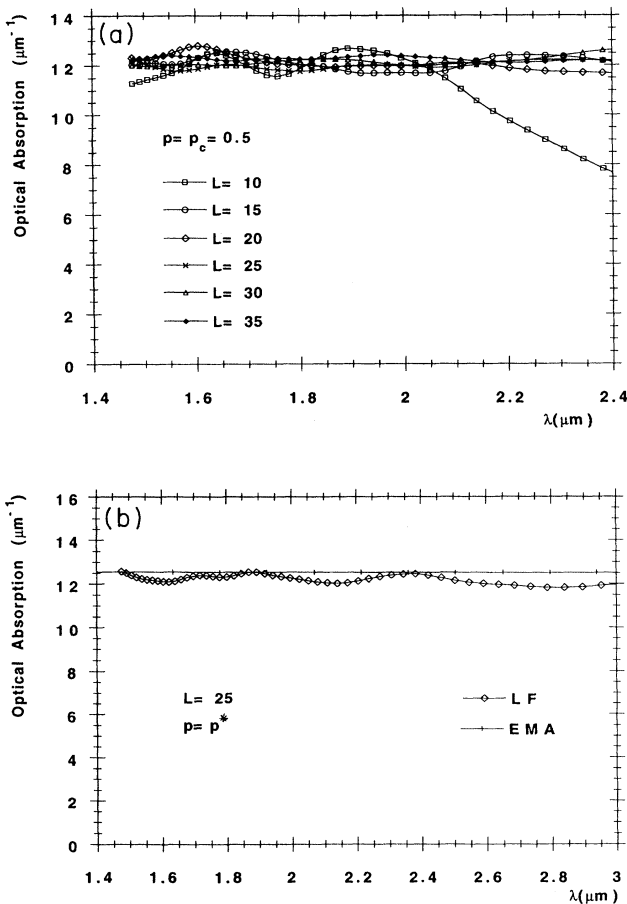


FIG. 3. (a) Near-infrared optical absorption, calculated with the FL algorithm for circuits of various linear size (from $L = 10$ to 35) as a function of wavelength for $p = 0.5$. (b) Near ir optical absorption, calculated with the FL algorithm for circuits of linear size $L = 25$ as a function of wavelength at the optical threshold p^* .

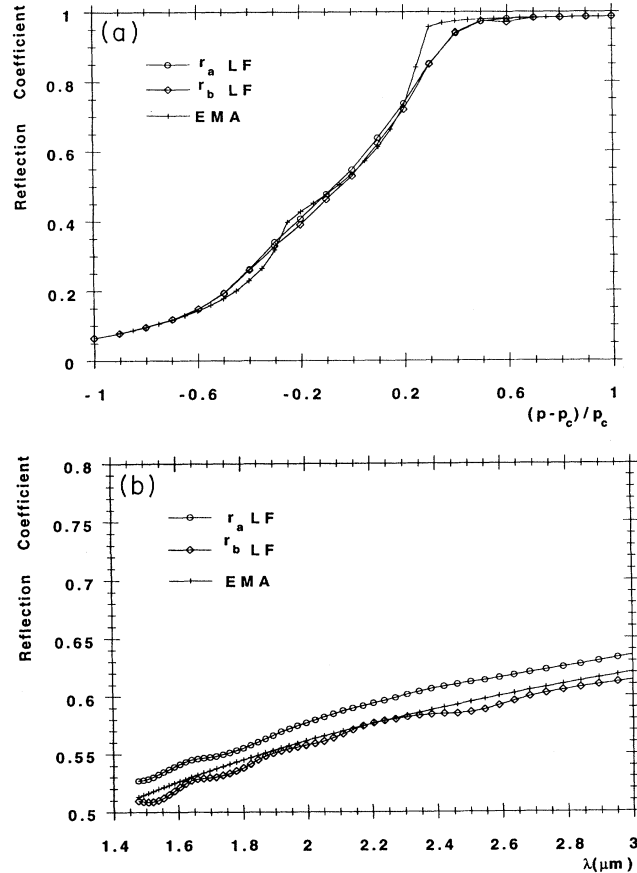


FIG. 4. (a) Reflection coefficient as a function of metal coverage for $\lambda = 1.7 \mu\text{m}$, calculated with the FL algorithm with two different averaging procedures for circuits of linear size 25 and compared with the results of the mean-field theory (EMA). (b) Reflection coefficient as a function of wavelength for $p = 0.5$ calculated with the FL algorithm with two different averaging procedures for circuits of linear size 25 and compared with the results of the mean-field theory (EMA).

fluctuations around the averaged values presented in Figs. 1–4 lie in a reasonable range and if the simulation method can reproduce the percolation critical exponents obtained by other methods. We have checked these two points.

(1) The largest fluctuations occur for ε_2 at $p \sim p_c$ and for $\text{Re}\Sigma$ in the tails of the cluster resonant modes region. In Fig. 5 we show the relative error on ε_1 at $p = p_c$ and the relative error on $\text{Re}\Sigma$ at $p = 0.25$ as a function of the linear size of the network. One can see that for L larger 20, provided one averages over a few thousand configurations, it is possible in both cases to achieve a result with a relative error smaller than 10%. All our results are in that range of precision.

(2) The FL method is able to yield percolation critical exponents with a high degree of accuracy. As an example and a way to check the performances of our program, we have plotted the variation of the log of the real part of Σ_{FL} vs $\log L$ for a circular frequency $\omega = 0.08\tau^{-1}$, where the conductivity still has its dc value, and found a value

of $t/\nu = 0.976 \pm 0.010$, which overlaps the range given by the Percola machine.²⁸

IV. COMPARISON WITH EXPERIMENTAL DATA

The FL simulations reported in this paper account qualitatively for the experimental features discussed in points 1 to 3 of the Introduction. A quantitative comparison with experimental optical data for various metal based composite can be done by adjusting the following parameters: τ^{-1} and ω_p , which depend on the mean free path, the effective depolarization factor g , which depends on the cluster morphology and determines the percolation threshold, which in most films and composite is larger than the percolation theory value. The dielectric constant ε_d and ε_m are modified by the intercluster capacitance due to surface charges. The effective value to be used for ε_d must also take account of the fact that the substrate fills part of the intergrain space as this has been demonstrated by hopping and tunneling conductivity studies at low metal coverage.²⁹ In our simulations the Au film optical conductivity close to p_c in the 1.5–2.2 μm range is $13 \mu\text{m}^{-1}$ compared to $22 \mu\text{m}^{-1}$ obtained from ellipsometric measurements by Gadenne, Beghadi, and Lafait.^{5,7} Since the optical conductivity at p_c scales as $\sqrt{\varepsilon_d}$, it is possible to reproduce the Gadenne data by assuming a higher value of ε_d to account for these capacitance effects. To compare with the p variation of the absorptance defined as $A = 1 - R - T$, where R and T are the reflectance and the transmittance, one has to remember that the thickness of the film increases with p . This explains why the absorptance is a continuously decreasing function for $p > p^*$ in contrast to the optical absorption coefficient, which increases outside the cluster absorption region towards its pure metal value (Fig. 1). To calculate the transmittance and the reflectance of the films from the reflection coefficient for a semi-infinite medium calculated and shown in Fig. 4, one has to consider the effect of multiple reflections due to the finite thickness of the film. This has been established by Abelès.²⁴ When the film thickness t is much smaller than the wavelength, these effects can be approximated to second order in t/λ by the following formulas:^{5,30}

$$R \approx \frac{(n_0 - n_s)^2 + (n_s - n_0)p + q}{(n_0 + n_s)^2 + (n_s + n_0)p + q}, \quad (4)$$

$$T \approx \frac{4n_0n_s}{(n_0 + n_s)^2 + (n_s + n_0)p + q},$$

with $p = 2\varepsilon_2\eta$ and

$$q = [\varepsilon_1^2 + \varepsilon_2^2 - (n_0^2 + n_s^2)\varepsilon_1 + n_0^2n_s^2]\eta^2,$$

where $\eta = 2\pi t/\lambda$ and n_0 and n_s are the refractive index of the air and the substrate⁵ ($n_s \sim 2$).

Figures 6 and 7 show the optical absorption coefficient, the reflection coefficient r , the absorptance A , reflectance R , and transmittance T as a function of the filling factor p and the wavelength at the optical threshold p^* . A , R , and T have been calculated with the exact Abelès equations. We have checked that the approximate formulas

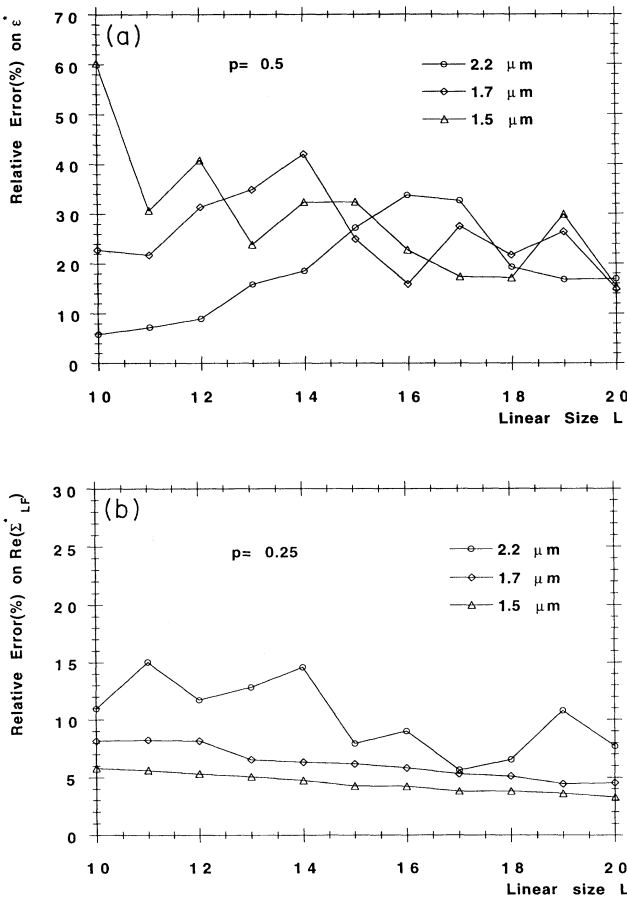


FIG. 5. (a) Relative error on ε_1 as a function of the circuit linear size calculated with the FL algorithm for three ir wavelengths at $p = 0.5$ and averaged over 10 000 samples. (b) Relative error on $\text{Re}\Sigma$ as a function of the circuit linear size calculated with the FL algorithm for three ir wavelengths at $p = 0.25$ and averaged over 10 000 samples.

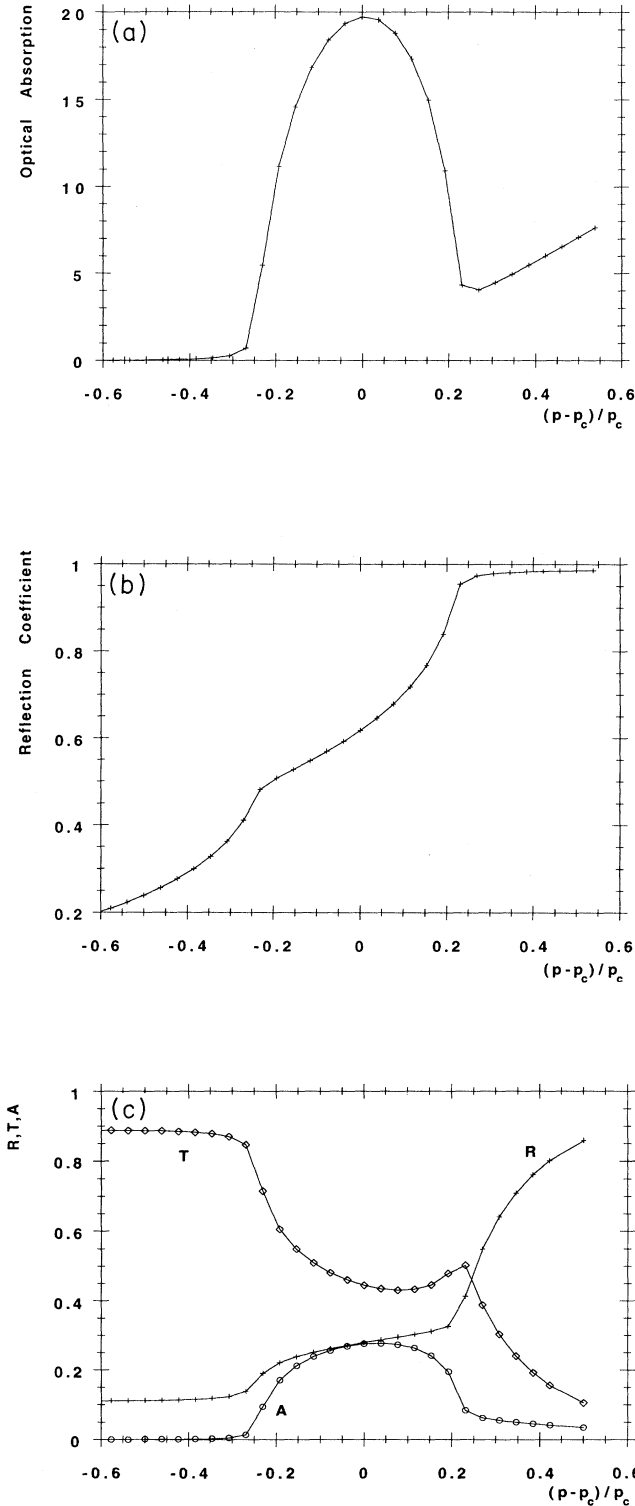


FIG. 6. (a) Optical absorption of an EMA model of gold granular model as a function of metal coverage. (b) Reflection coefficient of an EMA model of gold granular model as a function of metal coverage. (c) Absorptance, transmittance, and reflectance of an EMA model of gold granular thin film as a function of metal coverage.

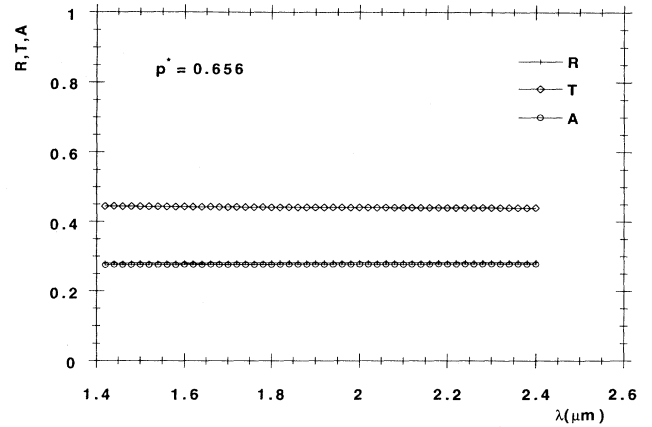


FIG. 7. Absorptance, transmittance, and reflectance of an EMA model of gold granular thin film at the optical threshold as a function of wavelength.

(4) are exact to less than 1% in the wavelength range considered. We have used the model of Sec. II with two small differences dictated by the physics of the problem. We have chosen a depolarization factor $g = 0.65$ compatible with the experimental percolation threshold and an insulator dielectric constant close to that of the substrate ($\epsilon_d = 4$). The film thickness is 100 \AA at p_c , a typical value reported in experimental papers. In the vicinity of p_c the agreement with experimental data^{5,7,12,13} is remarkable. A fine tuning involving the various parameters of the model could be used to fit exactly the observation but at this point would be irrelevant. Particularly noteworthy is the complete frequency independence of the three optical quantities A , R , and T at the optical threshold p^* . This result confirms the conclusions of paper I and the speculation on a direct relation between metal-insulator transition and the frequency independence of the optical properties.

V. DISCUSSION AND CONCLUSIONS

The simulation calculations we have performed have confirmed our findings¹⁴ that the good-bad conductor scaling law of Efros and Shklovskii¹⁸ and Straley¹⁹ are obeyed in 2D by the EMA and yields a frequency independence of the optical properties in the neat ir close to p_c but, more surprisingly, the good agreement in the anomalous absorption region leads to the conclusion that the analytical scaling functions used to represent the conductivity of a binary system with two conductivities $\sigma_d(\omega)$ and $\sigma_m(\omega)$ in the critical region can be approximated by the analytical scaling function obtained in the EMA. Indeed as discussed in Refs. 3 and 14, in the critical region around p_c the conductance scales as

$$\Sigma(\omega) = \sigma_m(\omega) |\Delta p|^t |\Phi_{\pm}(h(\omega)) |\Delta p|^{-s-t}|, \quad (5)$$

with $h(\omega) = \sigma_d(\omega) / \omega_m(\omega)$. The functions $\Phi_{\pm}(z)$ have the analytic properties compatible with the dc limits of

$\text{Re}(\Sigma)$ and $\text{Im}(\Sigma)$. The exponents t and s are the conductivity and superconductivity critical exponents. For $\tau^{-1} < \omega < \omega_p$, which is the frequency range of interest here and at the percolation threshold ($\Delta p \rightarrow 0$), the expression (5) gives $\phi_{\pm}(z) = Kh^u$ and $\Sigma(\omega) = K\sigma_m(\omega)h^u$ with $u = t/(s+t)$. K is a constant assumed to be universal. In two dimensions $s = t$ and $u = \frac{1}{2}$ as in the EMA. In the EMA where $\phi_{\pm}(z)$ can be calculated exactly^{14,16} $K = \sqrt{p_c/(1-p_c)}$. Our simulation calculations suggest that in the critical region $\phi_{\pm}(z)$ can be approximated by the analytical scaling function obtained in the EMA. This is what some authors^{26,31} have done implicitly by introducing without theoretical justification, the exact critical exponents t and s in the EMA equations to analyze the optical spectra of metal-insulator cermets. Our results give some solid ground to that assumption.

If the agreement between FL simulations and EMA is exceptionally good near p_c , as reported in Sec. IV there is a discrepancy in the region $\Delta p = \pm 0.25$ between EMA on one hand and simulation calculations and experimental data on the other hand. This is due to the inability of the EMA to deal with the tails of the cluster modes distribution and to the narrowing of the distribution width. This discrepancy already noted by other authors¹¹ has led them to believe that the EMA is inappropriate in the whole region -0.25 ± 0.25 . A similar phenomena appears in other disordered systems problems. In disordered alloys for instance, the electronic spectrum of electronic or vibration states calculated in the EMA (in that context, the coherent-potential approximation) is narrower than the actual one and cannot account for the Lifshitz tails states responsible for localization.³² The difference of width can be calculated from the study of the conductors scaling laws. One has from Ref. 3

$$|p_b - p_c| \approx |h|^{1/(s+t)} \quad (s = t = 1.3). \quad (6)$$

In the EMA one has $|p_b^{\text{EMA}} - p_c| \approx |h|^{1/2}$ with

$$h(\omega) = \frac{\sigma_m(\omega)}{\sigma_d(\omega)} \approx \frac{\varepsilon_d(\omega)}{-(\omega_p^2/\omega^2) + \varepsilon_m(\infty)}$$

in the near ir relevant wavelength range. Using these expressions, one finds that for $\lambda = 1.7 \mu\text{m}$, the bounds $(p_b - p_c)/p_c = \pm 0.431$ in the percolation theory and ± 0.272 in the EMA. These estimations are in excellent accord with the curves of Fig. 1. In the second case for

lower relative concentrations, one observes in the FL results the contributions of the Lifshitz tails. The agreement between these theoretical predictions and the numerical results is another proof of the power of the method and of the coherence of our interpretation of the films optical data.

In conclusion, we have shown that the broaden spectrum of Mie resonances is still playing an important role in the near ir absorption and reflectivity (in the range 2200–1500 nm) of granular thin films and give a plausible interpretation of the so-called anomalous absorption in complete agreement with the two conductivities scaling laws of the theory of percolation. These scaling laws do not rely on the exact morphology of the metallic clusters. This is very fortunate since, it is now obvious that the morphology of thin films is rather different from the cluster morphology of the classical theory of percolation.³³

Near the percolation threshold, the cluster resonant modes dominate the absorption and are not affected by size effects. Above p_c , the contribution of percolating electrons which obey the usual dc percolation scaling laws is too small to affect the behavior of the optical absorption. The results of the simulations confirm the calculations of paper I that the frequency independence of the optical properties in the near ir at the optical threshold p^* . The last, somehow unexpected, result is that the universal scaling function $\phi_{\pm}(z)$ might be well approximated by the scaling function of the mean-field theory. This justifies the efforts of Lafait and co-workers^{1,27,32} to interpret cermets data with the EMA expressions and the exact percolation theory exponents s and t . Formula (6) provides another method of extracting these exponents from experimental data. It would be interesting to study the change of the anomalous absorption width and therefore of t and s as one goes from a 2D to a 3D regime where the good agreement between simulation and EMA near p_c is expected to be lost.

ACKNOWLEDGMENTS

We acknowledge with thanks fruitful discussions with Dr. J. M. Luck, Dr. J. Lafait, Dr. P. Gadenne, Dr. M. Octavio, Dr. C. J. Lobb, and Dr. B. Souillard. This work has been supported by the programme "multimatériaux" of the Wallon Region and the programme "Tournesol" of the French Community of Belgium.

*Permanent address: Ecole Normale Boîte Postale No. 4288, Antananarivo, Madagascar.

†Permanent address: Laboratoire d'Énergétique E.E.S. Sciences Boîte Postale No. 906, Antananarivo, Madagascar.

¹J. Lafait, S. Berthier, M. Gadenne, and P. Gadenne, in *Physical Phenomena in Granular Materials*, edited by G. C. Cody *et al.*, MRS Symposia Proceedings No. 195 (Materials Research Society, Pittsburgh, 1990), p. 77.

²U. Kreibitz, M. Quiten, and D. Schoenauer, *Physica A* **157**, 244 (1989).

³J. P. Clerc, G. Giraud, J. M. Laugier, and J. M. Luck, *Adv.*

Phys. **39**, 191 (1990).

⁴R. W. Cohen, G. D. Cody, M. D. Coutts, and B. Abeles, *Phys. Rev. B* **8**, 3689 (1973).

⁵P. Gadenne, Thèse d'état, Université Paris VI, 1986.

⁶K. H. Khan, G. A. Niklasson, and C. G. Granqvist, *J. Appl. Phys.* **64**, 3327 (1988); M. Kunz, G. A. Niklasson, and C. G. Granqvist, *ibid.* **64**, 3740 (1988).

⁷P. Gadenne, A. Beghadi, and J. Lafait, *Opt. Commun.* **65**, 17 (1988).

⁸E. Dobierzewska-Mozrzyms and P. Bieganski, *Surf. Sci.* **200**, 417 (1988).

- ⁹M. Gajdardziska-Josifovska, R. C. McPhedran, D. R. McKenzie, and R. E. Collins, *Appl. Opt.* **28**, 2744 (1989).
- ¹⁰Y. Yagil and G. Deutscher, *Appl. Phys. Lett.* **52**, 373 (1988).
- ¹¹T. Robin and B. Souillard, *Opt. Commun.* **71**, 15 (1989).
- ¹²P. Gadenne, Y. Yagil, and G. Deutscher, *J. Appl. Phys.* **66**, 3019 (1989).
- ¹³Y. Yagil, M. Yosefin, D. J. Bergman, G. Deutscher, and P. Gadenne, *Phys. Rev. B* **43**, 11 342 (1991).
- ¹⁴F. Brouers, J. P. Clerc, and G. Giraud, in *Physical Phenomena in Granular Materials*, edited by G. C. Cody *et al.*, MRS Symposia Proceedings No. 195 (Materials Research Society, Pittsburgh, 1990), p. 77.
- ¹⁵F. Brouers, *Physica A* **157**, 454 (1989).
- ¹⁶F. Brouers, J. P. Clerc, and G. Giraud, *Phys. Rev. B* **44**, 5299 (1991).
- ¹⁷G. A. Niklasson and C. G. Granqvist, *J. Appl. Phys.* **55**, 3382 (1984); D. A. Bruggeman, *Ann. Phys. (Leipzig)* **24**, 636 (1935); R. Landauer, in *Electrical Transport and Optical Properties of Inhomogeneous Media*, (Ohio State University, 1977), Proceedings of the First Conference on the Electrical Transport and Optical Properties of Inhomogeneous Media, edited by J. C. Garland and D. B. Tanner, AIP Conf. Proceedings No. 40 (AIP, New York, 1978), pp. 2–43.
- ¹⁸E. L. Efros and B. I. Shklovskii, *Phys. Status Solidi B* **76**, 475 (1976).
- ¹⁹J. P. Straley, *J. Phys. C* **9**, 783 (1976).
- ²⁰J. M. Luck, *Phys. Rev. B* **43**, 3933 (1991).
- ²¹C. J. Lobb and D. J. Frank, *Phys. Rev. B* **30**, 4090 (1984).
- ²²X. C. Zeng, P. M. Hui, and D. Stroud, *Physica A* **157**, 370 (1989).
- ²³D. Stroud and P. M. Hui, *Phys. Rev. B* **37**, 8719 (1988); X. C. Zeng, P. M. Hui, and D. Stroud, *ibid.* **39**, 1063 (1989); X. C. Zeng, D. J. Bergman, P. M. Hui, and D. Stroud, *ibid.* **39**, 13 224 (1989).
- ²⁴F. Abelès, *Ann. Phys. (Paris)* **5**, 777 (1950).
- ²⁵D. J. Frank and C. J. Lobb, *Phys. Rev. B* **37**, 302 (1988).
- ²⁶S. Berthier, *Ann. Phys. (Paris)* **13**, 503 (1988).
- ²⁷J. Lafait, S. Berthier, and L. E. Regalado (unpublished).
- ²⁸J. M. Normand, H. J. Herrmann, and M. J. Hajjar, *Stat. Phys.* **52**, 441 (1988).
- ²⁹G. Desrousseaux, J. Trompetee, R. Faure, H. Schaffar, and J. P. Dussaulcy, *Thin Solid Films* **98**, 139 (1982).
- ³⁰F. Abelès, in *Advanced Optical Techniques*, edited by A. C. S. Van Heel (North-Holland, Amsterdam, 1967).
- ³¹S. Berthier, K. Driss-Khodja, and J. Lafait, *J. Phys. (Paris)* **48**, 601 (1987).
- ³²F. Brouers and J. Franz, *Phys. Status Solidi B* **113**, 431 (1982).
- ³³S. Blacher, F. Brouers, and G. Ananthakrishna, *Physica A* **185**, 28 (1992).